# Science Impact of 282 K Operating Temperature: WFI Imaging and Spectroscopy

Christopher Hirata (POC), Matthew Penny
Version 3 – September 11, 2014 – DRAFT

## Contents



# 1 Introduction

This note considers the impact of a 282 K operating temperature on the WFIRST-AFTA science programs. It is based on the document prepared for the January 2014 NRC study by the SDT ("Sensitivity of AFTA Science Performance to Temperature," led by Neil Gehrels, David Spergel, and Christopher Hirata with input from the SDT). This document is however intended to be both more detailed than the January 2014 analysis (in the areas covered by its scope), and is updated to reflect other recent changes in the WFIRST-AFTA design.

The 282 K (48 °F) case considered here differs from the 2013 AFTA report baseline of 270 K (27 °F) and the minimum operating temperature under consideration of 250 K (−10 °F).

## 1.1 Scope

This document presently covers the HLS spectroscopic survey and imaging survey, and the microlensing survey. We want to cover the other science areas when this input is available.

# 2 Assumptions

The following assumptions were retained from previous iterations of the study:

- Telescope temperatures of 270 K and 282 K are assessed.
- Throughputs are based on the May 25, 2014 update from Dave Content.
- Dark current of 0.015 $e^-$/pix/s is assumed. Here the term "dark current" implies current generated inside the detector and does not include thermal infrared emission from other components (telescope or instrument).
- The standard detector read noise model is used: one sample every 5.65 s (100 kHz readout, using 32 channels of the H4RG-10 device; the increase relative to the theoretical 5.24 s for a $4096^2$ device is due to the interlacing of the guide window). Read noise is assumed to be at the requirement level of 20

$e^-$ per correlated double sample (CDS), with a correlated noise floor of 5 $e^-$ r.m.s. The super-Poisson variance in MULTIACCUM mode[1] is included.

- A primary and secondary mirror emissivity of 0.02286 per surface was assumed in the ETC input files. This includes the standard 2% emissivity of protected silver, plus a 2% contamination term distributed evenly among the optical surfaces. Because of the way the WFIRST ETC treats the stray light requirement, the calculation is equivalent to an emissivity that is 10% larger than this.[2] That is, the calculations are equivalent to assuming an emissivity per surface of 0.025.

- For thermal calculations we added +2 K was applied to the telescope temperature. That is, the "270 K" runs are actually at 272 K and "282 K" is actually evaluated at 284 K. This factor is intended to account for several miscellaneous effects that will increase the thermal backgrounds in WFIRST beyond the formal thermal emission in a rectangular filter. For example, a $\Delta\lambda/\lambda = 0.05$ width trapezoid-shaped cutoff is equivalent to an increase in temperature of +0.65 K. A smaller effect is that the variation of the temperature across the mirror surface. A variation of $\sigma_T = 1$ K r.m.s. results in an effective emission temperature increase of +0.037 K relative to the mean temperature of the mirror due to the nonlinearity of the intensity-temperature relation for an emissive surface.[3]

- Because we are now baselining 2.5 $\mu$m cutoff detectors, a warm telescope creates an additional thermal background due to filter red-leak (or imperfect out-of-band rejection: a small fraction of the telescope thermal radiation near 2.5 $\mu$m penetrates the filter). An out-of-band rejection of $10^{-4}$ for all filters is assumed.

- In the F184 filter, microlensing-wide filter, and grism modes, a full pupil mask is assumed.[4] A pupil mask was not included for the H band in the 270 K baseline, but is recommended at 282 K; H band parameters reported herein at 282 K assume a pupil mask unless otherwise indicated. In the other filters, the secondary mirror support tubes are visible from the detector and their thermal emission (including red leak) is included, assuming that they contribute 6% of the beam solid angle as seen by the detector. (That is, the total emissivity is increased by 0.06.) A further increase of $0.31^2/(1-0.31^2) = 0.106$ is also included due to the central obstruction (where the detector sees a black telescope baffle). This is of course based on the assumption that the primary and secondary baffles will run at the same temperature at the telescope (270 or 282 K) – this is probably over-conservative.[5]

- Internal instrument backgrounds of 0.012 $e^-$/p/s (corresponding to placing the detector in a 152 K blackbody) are assumed, independent of the chosen telescope temperature.

- Zodiacal backgrounds are computed according to the model in the ETC. The 2013 baseline assumptions for the HLS are 1.3× the zodiacal background at the ecliptic poles.

- The ETC does **not** take into account the variation of the filter bandpass with angle of incidence; it is assumed here that the filter bandpasses specified correspond to the center of the field (chief ray normal on the filter). As one approaches the edges of the field the filter shifts slightly blueward. This will result in the thermal background in the reddest filters and the grism mode showing a maximum near the field center and a decrease toward the edges. This effect is not discussed in this document (which is concerned with the overall level of thermal emission) but will be of interest for calibration and survey selection function applications.

[1] See Eq. (1) of B. Rauscher *et al.*, *Proc. Astron. Soc. Pac.* **119**:768 (2007).

[2] Stray light is not explicitly included in the WFIRST ETC, but there are separate throughput tables for "signal" and "noise." To account for stray light at the 10% requirement level, the "noise" throughput table was increased by +10%.

[3] Like most scatter-rectification effects, this effect scales quadratically with $\sigma_T$.

[4] Pupil masks are mounted on the filter/element wheel, so a different geometry can be chosen for each filter.

[5] The thermal environment seen by these baffles is dominated by the black interior of the OBA, rather than the reflective mirrors. It is thus likely that they will run at lower temperature than the telescope.

# 3 HLS spectroscopy

An example set of HLS spectroscopy forecasts were performed using the 2013 SDT report model for the H$\alpha$ luminosity function (based on the HST/WFC3 results[6]). This assessment assumes exposures of $t = 344.65$ s (61 frames) and zodiacal background at the reference level (1.3× at the poles), and a Galactic dust column of $E(B-V) = 0.035$. The default wavefront error assumed is 200 nm r.m.s., near the center of the range under consideration as a requirement (150—240 nm).

Table 1 explores the possible changes in the survey parameters, with a reference case ("`REF`") at 270 K. The subsequent cases are as follows:

- The `282` case increases the telescope temperature to 282 K.
- The `282B` case is also at 282 K, but mitigates the thermal background by reducing the red cutoff from 1.95 $\mu$m to 1.90 $\mu$m.
- The `282BI` case is equivalent to the `282B` case, except that the wavefront budget is tightened from 200 nm r.m.s. to 150 nm r.m.s.
- The `282BW` case is equivalent to the `282B` case, except that the wavefront budget is loosened from 200 nm r.m.s. to 240 nm r.m.s.

Note that in the `282B` case the thermal background is a significant but not dominant contributor to the current in the detectors. The zodiacal light contributes 0.43 $e^-$/p/s, as compared to telescope thermal emission, which contributes 0.26 $e^-$/p/s. The contribution of the telescope thermal emission to the overall noise variance is ∼30%. The `282BI` and `282BW` cases differ only in wavefront error and hence have identical thermal backgrounds.

The reduced bandpass of the "B" cases results in the loss of H$\alpha$ emitters at the highest end of the redshift range, which has a modest negative impact on the science. However the total number of galaxies observed is only 11% lower than the `REF` case. This difference is similar to the impact of other choices in the mission such as the grism mode wavefront error budget.

# 4 Imaging surveys

The impact of the higher telescope operating temperature is most significant in the F184 band (1.683—2.000 $\mu$m) as this is the reddest of the imaging filters. The H filter (1.380—1.774 $\mu$m) was also examined here because it experiences an elevated thermal background without the full pupil mask. The bluer filters (J and Y) are less affected than H. **It is recommended that if we operate the telescope at 282 K, then the full pupil mask should be included for the H band** since this leads to greater depth and number density of galaxies than accepting the thermal emission of the baffles and spider.

Imaging exposure times are shown in Table 2. For long exposures, e.g. to reach 28 mag AB, the H band experiences a time penalty of 9%, whereas the F184 filter experiences a time penalty of 2.2×. (This penalty is effectively saturated at 28 mag AB since Poisson noise dominates over read noise in these long exposures.) For shorter exposures, the F184 filter suffers less degradation because of the significant contribution of read noise: e.g. at 26.1 mag AB, the time penalty for the higher telescope temperature is 41%.

## 4.1 The HLS imaging survey

The planned HLS exposure time is 5 × 180.8 s = 904 s (i.e. 32 frames in each of 5 exposures). In the F184 filter, the predicted depth under reference conditions for point sources ($5\sigma$ detection) is 26.13 mag AB (270 K) or 25.83 mag (282 K): this is a degradation of sensitivity of **0.30 mag**. We consider point source sensitivities here; WFIRST is less sensitive to extended sources, but the temperature dependence of the

[6] J. Colbert *et al.*, *Astrophys. J.* **34**:16 (2013). The SDT report was based on a pre-publication version, arXiv:1305.1399v1.

Table 1: The galaxy redshift survey yields for the cases described in the text. The "total" row at the bottom is the total number of galaxies per deg$^2$. For the sake of comparison of the columns, extra significant figures are given, but remember that the absolute number density of H$\alpha$ emitters is uncertain by a factor of $\sim 2$. The columns indicate variations of the cases. The last row is the change in the total number of galaxies relative to the `REF` case. Note that all of the cases except for the first are at 282 K.

| $z$ | $dN/dz/dA$ [gal/deg$^2$/($\Delta z = 1$)] | | | | |
|---|---|---|---|---|---|
| | `REF` | `282` | `282B` | `282BI` | `282BW` |
| $z_{\mathrm{H}\alpha}$ range | 1.06—1.97 | 1.06—1.97 | 1.06—1.88 | 1.06—1.88 | 1.06—1.88 |
| 1.10 | 9945 | 6957 | 9319 | 10326 | 8485 |
| 1.15 | 11830 | 8450 | 11126 | 12281 | 10152 |
| 1.20 | 13635 | 9904 | 12863 | 14149 | 11755 |
| 1.25 | 14721 | 10785 | 13908 | 15267 | 12713 |
| 1.30 | 15288 | 11246 | 14455 | 15843 | 13205 |
| 1.35 | 15808 | 11671 | 14956 | 16365 | 13655 |
| 1.40 | 16031 | 11855 | 15171 | 16576 | 13839 |
| 1.45 | 16103 | 11915 | 15241 | 16633 | 13894 |
| 1.50 | 16043 | 11871 | 15184 | 16574 | 13851 |
| 1.55 | 15026 | 11022 | 14199 | 15540 | 12928 |
| 1.60 | 14070 | 10230 | 13274 | 14566 | 12065 |
| 1.65 | 13035 | 9384 | 12277 | 13510 | 11139 |
| 1.70 | 11988 | 8538 | 11269 | 12438 | 10208 |
| 1.75 | 10849 | 7627 | 10174 | 11269 | 9200 |
| 1.80 | 9647 | 6681 | 9023 | 10034 | 8143 |
| 1.85 | 8510 | 5798 | 7936 | 8862 | 7149 |
| 1.90 | 7282 | 4861 | 0 | 0 | 0 |
| 1.95 | 6006 | 3909 | 0 | 0 | 0 |
| total | 11263 | 8117 | 10019 | 11012 | 9119 |
| change | nil | $-28\%$ | $-11\%$ | $-2\%$ | $-19\%$ |

sensitivity (in number of magnitudes of degradation) is the same regardless of the size and morphology of the source as long as we are considering faint sources where the background noise dominates over Poisson fluctuations in photons from the source.[7]

The loss of only 0.30 mag of depth in F184 when going from 270 K to 282 K may seem counterintuitive since the telescope thermal emission (which is brighter than the zodiacal emission) increases by a factor of 3.2×. It is therefore instructive to review the intermediate results of the ETC to understand why only a modest degradation is predicted.

- The sky background (including zodiacal light and the 10% stray light factor) is 0.26 $e^-$/p/s, or 48 $e^-$/p in a 180.8 s exposure.
- The telescope thermal background rate (or total in an exposure) at 270 K is 0.37 $e^-$/p/s (67 $e^-$/p), and at 282 K is 1.18 $e^-$/p/s (213 $e^-$/p).
- The read noise model at 20 $e^-$ r.m.s. per CDS gives a total read noise variance of $\sigma^2 = 100\ (e^-)^2$. Based on prior experience with previous WFIRST designs, it is typical for read noise to be more important than sky Poisson noise in fast imaging surveys with medium-width (in this case $\lambda/\Delta\lambda = 5.8$) filters.
- The total noise variance budget at 282 K is 420 $(e^-)^2$/ per pixel. The telescope thermal background contributes 61% of this. At 270 K the noise variance would have been 244 $(e^-)^2$ per pixel, of which 33% is telescope thermal emission.

Note that the statement in the NRC report[8] that "the low margin stems from the fact that the sensitivity is completely dominated by the telescope mirror temperature" is not correct at the 270 K baseline temperature or even the 277.6 K minimum of the qualified range, and is only marginally true at 282 K (and even then only in the F184 filter). In fact, read noise, zodiacal light, and telescope thermal emission all play significant roles in the noise budget.[9]

The H band also contains some thermal emission, and in fact without the pupil mask in H band observations the detector sees the secondary mirror support tubes and central baffle that are masked in the F184 or grism modes. The sky background in H band for reference conditions is 0.45 $e^-$/p/s, as compared to telescope thermal backgrounds of 0.12 $e^-$/p/s (270 K, no mask) or 0.08 $e^-$/p/s (282 K, with mask). This has roughly equal contributions from the mirrors (which have low emissivity and high solid angle) and the baffles and struts (which have high emissivity and low solid angle). The consequences of this are that the H band $5\sigma$ point source sensitivity worsens from 26.71 mag AB (270 K, no mask) to 26.63 mag AB (282 K, with mask). The implied reduction in effective shape number density $n_{\rm eff}$ for the weak lensing program is −5% in the H band.[10]

# 5 Microlensing

The microlensing survey uses primarily the wide filter (W149), which due to the cutoff at 2 $\mu$m admits a significant thermal background. However, since microlensing observations are performed close to the ecliptic[11] (a "typical" ecliptic latitude is −5°), the sky background is also higher. At the median of the microlensing survey (observation direction 90° from the Sun), we estimate a zodiacal count rate of 3.28 $e^-$/p/s, in comparison to the thermal emission count rate of 1.21 $e^-$/p/s (at 282 K) or 0.39 $e^-$/p/s (at 270 K). The thermal rate, while significant, is not dominant even at the higher temperature.

[7] In F184, for an $r_{1/2} = 0.3$ arc sec source with an exponential profile the sensitivity is 1.05 mag worse than for a point source.

[8] National Research Council, *Evaluation of the Implementation of WFIRST/AFTA in the Context of New Worlds, New Horizons in Astronomy and Astrophysics*. Washington, DC: The National Academies Press, 2014.

[9] It is true that with a colder telescope (≤ 270 K) there would be more to gain by improving detector characteristics such as read noise than at 282 K. However such opportunities are not how we normally assess margin.

[10] These parameters are 26.58 mag AB and −8% weak lensing source losses if no pupil mask is assumed in the H band.

[11] This is a coincidence, based on the fact that the Galactic Center is currently near the Ecliptic Plane.

Table 2: The imaging exposure times in seconds in F184, H, and J bands to achieve the stated $5\sigma$ point source sensitivity in AB magnitudes. It was assumed that the total exposure would be split into 5 (F184,H) or 6 (J) separate sub-exposures. A zodiacal background of 1.3× the brightness at the ecliptic pole was assumed. Exposure times are quantized in units of frames.

| Lim. mag. | F184 | | H | | J | |
|---|---|---|---|---|---|---|
| | 270 K | 282 K | 270 K | 282 K | 270 K | 282 K |
| 25.0 | 367 | 395 | 254 | 254 | 271 | 271 |
| 25.1 | 395 | 423 | 254 | 282 | 305 | 305 |
| 25.2 | 423 | 452 | 282 | 310 | 305 | 339 |
| 25.3 | 452 | 508 | 310 | 310 | 339 | 339 |
| 25.4 | 480 | 565 | 310 | 339 | 372 | 372 |
| 25.5 | 508 | 621 | 339 | 367 | 406 | 406 |
| 25.6 | 565 | 706 | 367 | 395 | 406 | 406 |
| 25.7 | 621 | 791 | 395 | 423 | 440 | 440 |
| 25.8 | 678 | 875 | 423 | 452 | 474 | 474 |
| 25.9 | 734 | 988 | 452 | 480 | 508 | 508 |
| 26.0 | 819 | 1158 | 480 | 536 | 542 | 542 |
| 26.1 | 904 | 1327 | 536 | 565 | 576 | 610 |
| 26.2 | 988 | 1553 | 565 | 621 | 644 | 644 |
| 26.3 | 1101 | 1808 | 621 | 678 | 678 | 711 |
| 26.4 | 1243 | 2118 | 678 | 734 | 745 | 745 |
| 26.5 | 1412 | 2514 | 734 | 819 | 813 | 813 |
| 26.6 | 1610 | 2966 | 819 | 875 | 881 | 915 |
| 26.7 | 1864 | 3531 | 904 | 988 | 983 | 983 |
| 26.8 | 2147 | 4209 | 1017 | 1101 | 1050 | 1084 |
| 26.9 | 2514 | 5028 | 1130 | 1214 | 1186 | 1220 |
| 27.0 | 2938 | 6017 | 1271 | 1356 | 1288 | 1356 |
| 27.1 | 3474 | 7203 | 1412 | 1553 | 1457 | 1491 |
| 27.2 | 4096 | 8644 | 1610 | 1779 | 1627 | 1695 |
| 27.3 | 4859 | 10367 | 1864 | 2034 | 1830 | 1898 |
| 27.4 | 5763 | 12430 | 2147 | 2344 | 2067 | 2169 |
| 27.5 | 6893 | 14916 | 2486 | 2712 | 2373 | 2508 |
| 27.6 | 8220 | 17910 | 2909 | 3192 | 2745 | 2915 |
| 27.7 | 9831 | 21526 | 3418 | 3757 | 3186 | 3390 |
| 27.8 | 11780 | 25848 | 4039 | 4407 | 3695 | 3966 |
| 27.9 | 14096 | 31046 | 4774 | 5226 | 4339 | 4644 |
| 28.0 | 16921 | 37318 | 5678 | 6215 | 5085 | 5491 |

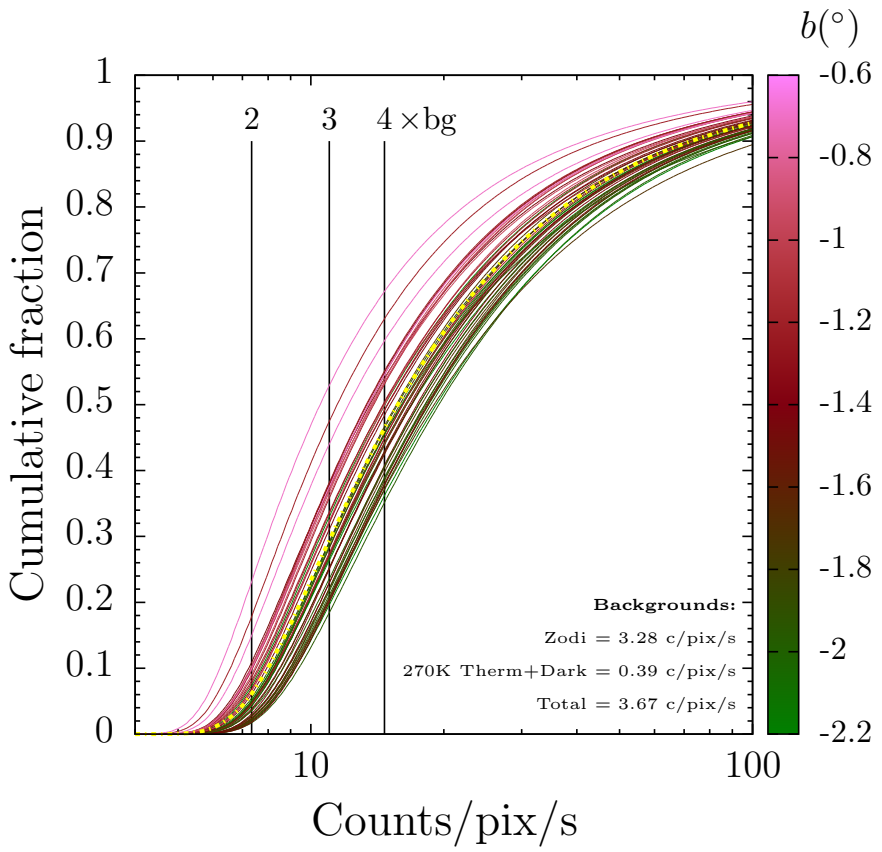


Figure 1: The simulated distribution of count rates from starlight + zodiacal background in the microlensing fields. Colors indicate fields at different Galactic latitudes; the yellow curve is the mean over all fields simulated.

In fact, in most pixels in the microlensing fields, the count rate is dominated not even by the zodiacal background but by starlight. The distribution of starlight count rates is shown in Figure 1. The median starlight count rate is 12.06 $e^-$/p/s; the Poisson error bar on the flux in a median brightness pixel is thus greater at 282 K than at 270 K by a factor of $\sqrt{(12.06 + 3.28 + 1.21)/(12.06 + 3.28 + 0.39)} = 1.026$, i.e there is a 2.6% degradation. The degradation due to the higher thermal background is worse for fainter pixels, e.g. at the 10th percentile brightness (4.32 $e^-$/p/s of starlight) the degradation worsens to 5.0%, and at the 1st percentile brightness (2.34 $e^-$/p/s of starlight) it worsens to 6.6%.

On the basis of this very minor degradation in the photometric uncertainties in the microlensing fields, we conclude that the higher operating temperature will have negligible impact on the WFIRST microlensing program.